WIDEBAND DUAL-LINEAR POLARIZED MICROSTRIP PATCH ANTENNA

A Thesis

by

CHRISTOPHER B. SMITH

Submitted to the Office of Graduate Studies of
Texas A&M University
in partial fulfillment of the requirements for the degree of

MASTER OF SCIENCE

December 2008

Major Subject: Electrical Engineering

WIDEBAND DUAL-LINEAR POLARIZED MICROSTRIP PATCH ANTENNA

A Thesis

by

CHRISTOPHER B. SMITH

Submitted to the Office of Graduate Studies of
Texas A&M University
in partial fulfillment of the requirements for the degree of

MASTER OF SCIENCE

Approved by:

Chair of Committee, Kai Chang
Committee Members, Robert D. Nevels
Hamid Toliyat
Raytcho Lazarov
Head of Department, Costas N. Georghiades

December 2008

Major Subject: Electrical Engineering

ABSTRACT

Wideband Dual-Linear Polarized Microstrip Patch Antenna. (December 2008)

Christopher B. Smith, B.S., Texas A&M University

Chair of Advisory Committee: Dr. Kai Chang

Due to the recent interest in broadband antennas a microstrip patch antenna was developed to meet the need for a cheap, low profile, broadband antenna. This antenna could be used in a wide range of applications such as in the communications industry for cell phones or satellite communication. Particle Swarm Optimization was used to design the dual-linear polarization broadband microstrip antenna and impedance matching network. This optimization method greatly reduced the time needed to find viable antenna parameters. A dual input patch antenna with over 30% bandwidth in the X-band was simulated using Ansoft's High Frequency Structural Simulator (HFSS) in conjunction with Particle Swarm Optimization. A single input and a dual input antenna was then fabricated. The fabricated antennas were composed of stacked microstrip patches over a set of bowtie apertures in the ground plane that were perpendicular to one another. A dual offset microstrip feedline was used to feed the aperture. Two different layers were used for the microstrip feedline of each polarization. The resulting measured impedance bandwidth was even wider than predicted. The antenna pattern was measured at several frequencies over the antenna bandwidth and was found to have good gain, consistent antenna patterns and low cross polarization.

ACKNOWLEDGEMENTS

I wish to thank Dr. Chang and Dr. Nevels for their help and guidance during my bachelor and masters degrees. I would like to thank Dr. Toliyat and Dr. Lazarov for serving as members on my thesis committee. I would also like to thank Raytheon for their support of my research and to the Advanced Circuits group for teaching me how to use HFSS in microwave design and apply the theory learned in school. Finally, I would like to thank my family, especially my wife, for their love, support, and patience.

TABLE OF CONTENTS

LIST OF FIGURES

FIGURE Page

CHAPTER I

INTRODUCTION

Recently there has been much interest in microstrip patch antennas. Because of their simplicity and compatibility with printed-circuit technology microstrip antennas are widely used in the microwave frequency spectrum. Simply a microstrip antenna is a rectangular or other shape, patch of metal on top of a grounded dielectric substrate. Microstrip patch antennas are attractive in antenna applications for many reasons. They are easy and cheap to manufacture, lightweight, and planar to list just a few advantages. Also they can be manufactured either as a stand-alone element or as part of an array. However, these advantages are offset by low efficiency and limited bandwidth. In recent years much research and testing has been done to increase both the bandwidth and radiation efficiency of microstrip antennas.

The main goals of this project are to overcome these disadvantages and to develop an antenna with the following characteristics:

- Operates in the X-band (8 to 12GHz) frequency range
- Has a bandwidth of 20 to 30%
- Lightweight
- Dual-Linear polarization and good polarization orthogonality at scan corners
- Low loss of input signal

This thesis follows the style and format of the *IEEE Transactions on Antennas and Propagation.*

Because the lower portion of the frequency spectrum (S and C bands) is becoming saturated there is a need to move to higher and higher frequency bands. Thus a microstrip patch antenna as described would be useful to utilize a higher portion of the frequency spectrum.

Additional characteristics that will be pursued if time permits include:

- Usable in an array with ±30 degrees by ±15 degrees scanning
- Antenna element that allows for sub-panel buildup for use in building arrays: planar, ideally no pins to align at each element, etc.
- Appropriate interface/balun structure to impedance match the antenna to the transmit/receive layer
- Compatibility with a facesheet for emissivity coatings and charge bleedoff

CHAPTER II

BACKGROUND

Recent research in numerical methods has led to mathematical models that allow for the advancement of microstrip patch antennas for use in higher frequency ranges. There are several important factors to consider in designing a broadband microstrip antenna. They include: the type and thickness of the antenna substrate, the method for feeding the antenna, size of patch antenna, polarization of antenna, the presence of slots in the patch and the use of fractal antennas.

II.1 IMPORTANT BROADBAND DESIGN PARAMETERS

Antenna Substrate. The thickness and type of substrate used determines the radiation characteristics of a patch antenna. The impedance bandwidth, which measures the radiation efficiency, depends upon its quality factor, also know as its Q. These two factors vary inversely to one another. A lower Q will therefore give an antenna with a wider bandwidth. The substrate used for the antenna has a large effect on the Q. The dielectric constant (ε_r) and substrate height (h) can be varied to obtain different Q. As seen in Figure 1, the efficiency is greater for low dielectric constant substrates, and, as the height is increased, the bandwidth also increases.

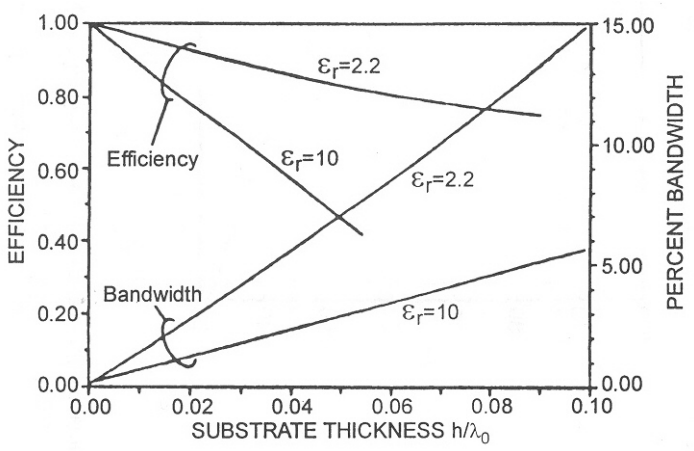

Figure 1: Efficiency and bandwidth versus substrate height at constant resonant frequency for rectangular microstrip patch. (Source: D. M. Pozar, "Microstrip Antennas," *Proc. IEEE*, Vol. 80, No. 1, January 1992. © 1992 IEEE).

Resonant Frequency. The patch length is a critical design parameter in the determination of the resonant frequency. Equation (1) shows how to determine the patch length L for the TM_{10} [1] mode in a rectangular patch antenna, where c and f_r are the speed of light and the resonant frequency respectively.

$$L = \frac{c}{2 \cdot f_r \cdot \sqrt{\varepsilon_r}} \qquad (1)$$

In Figure 1, it was noted that for greater height to wavelength ratios the bandwidth is increased. As the ratio is increased the fringing fields at the edge of the microstrip patch have a greater effect and should be taken into consideration. Equation (2) accounts for the fringing fields.

$$L = \frac{c}{2 \cdot f_r \cdot \sqrt{\varepsilon_{re}}} - 2 \cdot \Delta L \qquad (2)$$

Antenna Feed. Using thick substrates leads to difficulties in feeding the patch antenna. Two of the most common ways to feed the patch antenna would be to use a microstrip line or coaxial probe. The difficulty with a microstrip feed is that the characteristics that yield a desirable radiator make for a poor transmission line. Whereas the difficulty with the coaxial probe feed is a high inductive mismatch due to the long probe feed. To offset the inductance, a capacitance of some sort needs to be introduced. Another feed method that shows promise is aperture coupling. An aperture coupled feed has a slot cut into the ground plane below the patch antenna. The feed structure then couples to the patch through the aperture in the ground plane. The feed structure is some form of microstrip line on the opposite side of the ground plane from the antenna. By varying the shape of the aperture the coupling can be strengthened or weakened. Research has shown that the best coupling occurs for an aperture the shape of a bowtie [2].

No matter which method is chosen to feed the antenna, an appropriate feed location must be chosen so that the feed and the antenna may be properly impedance matched. The input impedance at the edge of a patch antenna can be found using Equation (3) [3]. The cosine squared factor is to reduce the input impedance when the feed is inset into the patch antenna. The Δx variable is the distance from the edge of the patch to the feed point. The other variables are the dielectric constant (ε_r), the antenna length (L) and width (W).

$$Z_A = 90 \cdot \frac{\varepsilon_r^{\,2}}{\varepsilon_r - 1} \cdot \left(\frac{L}{W}\right)^2 \cdot \cos^2\left(\frac{\pi \cdot \Delta x}{L}\right) \qquad (3)$$

Polarization. Another factor to consider in choosing the feed method and location is the polarization that is imposed upon the radiated electric field. Linear polarization is defined as "a time harmonic wave that at a given point in space the electric-field (or magnetic-field) vector at that point is always oriented along the same straight line at every instant of time."[4] In contrast, dual linear polarization is characterized by two orthogonal linear polarizations on the same antenna. Dual polarization antennas have the benefit of allowing two signals, with different orientations, to be broadcast or received on the same antenna.

Since both polarizations need to have their bandwidth at the same frequency, the orthogonal sides need to have the same length, which will lead to a patch antenna that is square. This design requirement has the negative effect of reducing the bandwidth of the antenna [14]. In a rectangular patch antenna a portion of the bandwidth is due to the ratio of the width over the length being greater than 1 but less than 2 [4].

Many designs have been proposed for dual linear polarized patch antennas that overcome the limitations imposed by microstrip technology. Numerous of these designs use an L-probe for one of the two input signals. The other input signal either uses another feeding technique or an additional L-probe. An L-probe is a coaxial probe that makes a 90 degree bend in the substrate instead of connecting physically with the

antenna. The figure below is an example of this [5]. There are also many other examples of broadband dual polarized antennas [6].

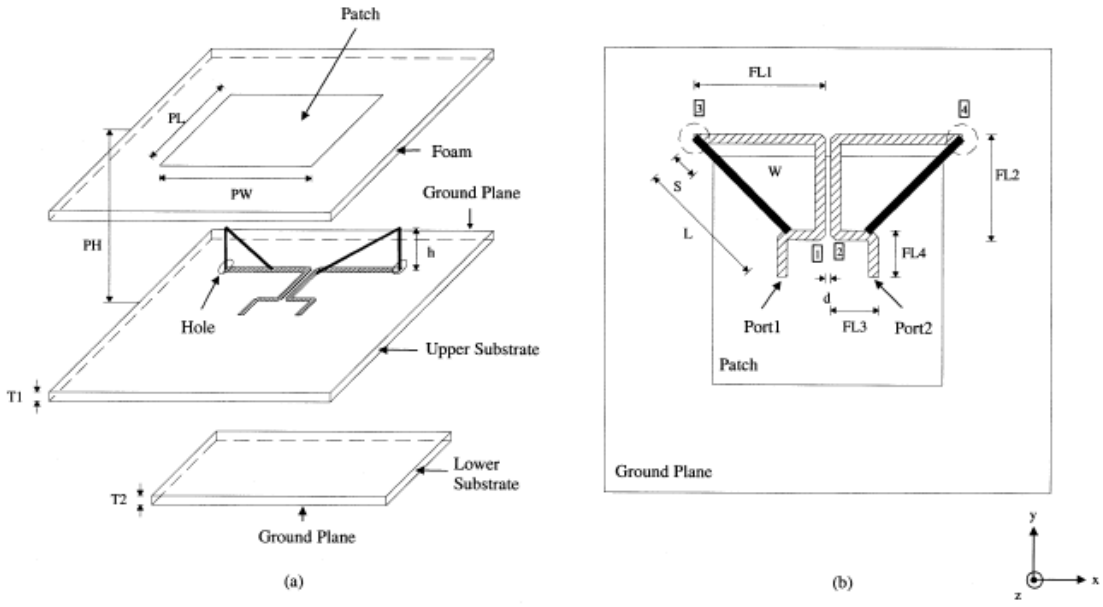

Figure 2: Geometry of a microstrip patch antenna with L-probes feeding the antenna. (© 2002 IEEE)

While using L-probes effectively increases the bandwidth of the antenna, antennas using L-probes in their design are difficult to manufacture due the L-probes geometry. This geometry leads to two problems. The first is that a more complex manufacturing process is more error-prone leading to lower manufacturing efficiencies. The second is that the process to produce a single device will be more expensive than a simpler process. The expense to produce this design may price it out of many applications that it might be used for. The easiest solution to this problem is to design an antenna that is less geometrically complex and therefore easier and cheaper to produce.

Patch Shape. Another method to increase the bandwidth of a patch antenna is to cut slots in the antenna [7]. These slots force the currents to flow another way and can have a salutary effect on the performance of the antenna. Because of the limitation imposed by dual polarization, any slots in the patch must be symmetric so as to act on both polarizations equally so the slots can allow the antenna bandwidth to be broader.

An alternative to the rectangular patch antenna is a fractal patch antenna. Fractal antennas use self similar geometry to focus the current over different regions of the antenna at different resonant frequencies. This leads to fractal antennas acting more as arrays at certain frequencies than as a single antenna. A Koch snowflake fractal patch antenna is tested and has a 1.5:1 VSWR bandwidth of 12% [8]. At certain frequencies the currents are focused in specific areas of the antenna and it has the appearance more of a 2x2 array than the single antenna it actually is. This is also shown for a Sierpinski gasket antenna [9]. Every time that the frequency doubles the active region of the Sierpinski antenna is reduced by a factor of two. Use of self similar geometry allows for antennas with a broader bandwidth.

The optimization of these parameters will allow for the advancement of dual-polarization antennas into the broadband antennas field. This will broaden the application of patch antennas because of its versatility and multi-functionality. It could be used in communication arrays allowing information to be sent and received simultaneously. It will also extend the understanding of thick substrate antennas in this area.

II.2 PARTICLE SWARM OPTIMIZATION

Particle Swarm Optimization (PSO) is an evolutionary computation method originally formulated by Eberhart and Kennedy in 1995. Even though this method is very simple to implement and has better performance than the popular Genetic Algorithm optimization method [10, 11], PSO has yet to receive a lot of attention from the electromagnetics community.

PSO is based on the observation that a swarm of insects, a flock of birds, a school of fish, or a herd of four legged animals behaves in a distinctive manner when searching for food, protection, or something else. When a member of the group sees a desirable path, the rest of the group will often follow soon afterwards. Each member is constantly searching its locality for the best and learns by experience. Each member is also learning from the others in the group, generally from whoever is the best performer.

The method of PSO emulates the behavior mentioned [12]. Each member or particle of the group or swarm has a position and velocity in multidimensional space. This multidimensional space represents the solution space that is being searched. Each dimension represents one variable in the problem to be solved so each particle's position is a solution of the problem. Every member remembers the best position they have visited as they move through multidimensional space. The members also communicate with one another and compare the best positions that each has found and then adjust their position and velocity based on the good positions found. There are two ways that this communication occurs, and normally only one is used. The first is that everyone

compares their positions and the best position in the whole swarm is picked; this global best position is known by all particles. The second is that subsets of the swarm called neighborhoods compare their best positions for the selection of the best position for the subset; this is known as the local or neighborhood best position.

The idea of a neighborhood has nothing to do with members' proximity to one another in multidimensional space. A neighborhood is generally defined prior to the commencement of the search. A simple example of a neighborhood would be a circular one. Suppose that there are 10 particles in a swarm and each particle has two neighbors. The 4^{th} particle would have as its neighbors particles 3 and 5. These three particles would compare notes as to their best position. The benefit of using a neighborhood best position rather than a global best position is that the knowledge of the currently known best position is slowly promulgated through the swarm. This allows time for other neighborhoods to continue searching the best positions that they have seen, and this permits the swarm to avoid being pulled into local minimas or maximas. Conversely if another global best exists between the current global best and a neighborhood that has not seen this current best position, then the odds are higher that it will be found.

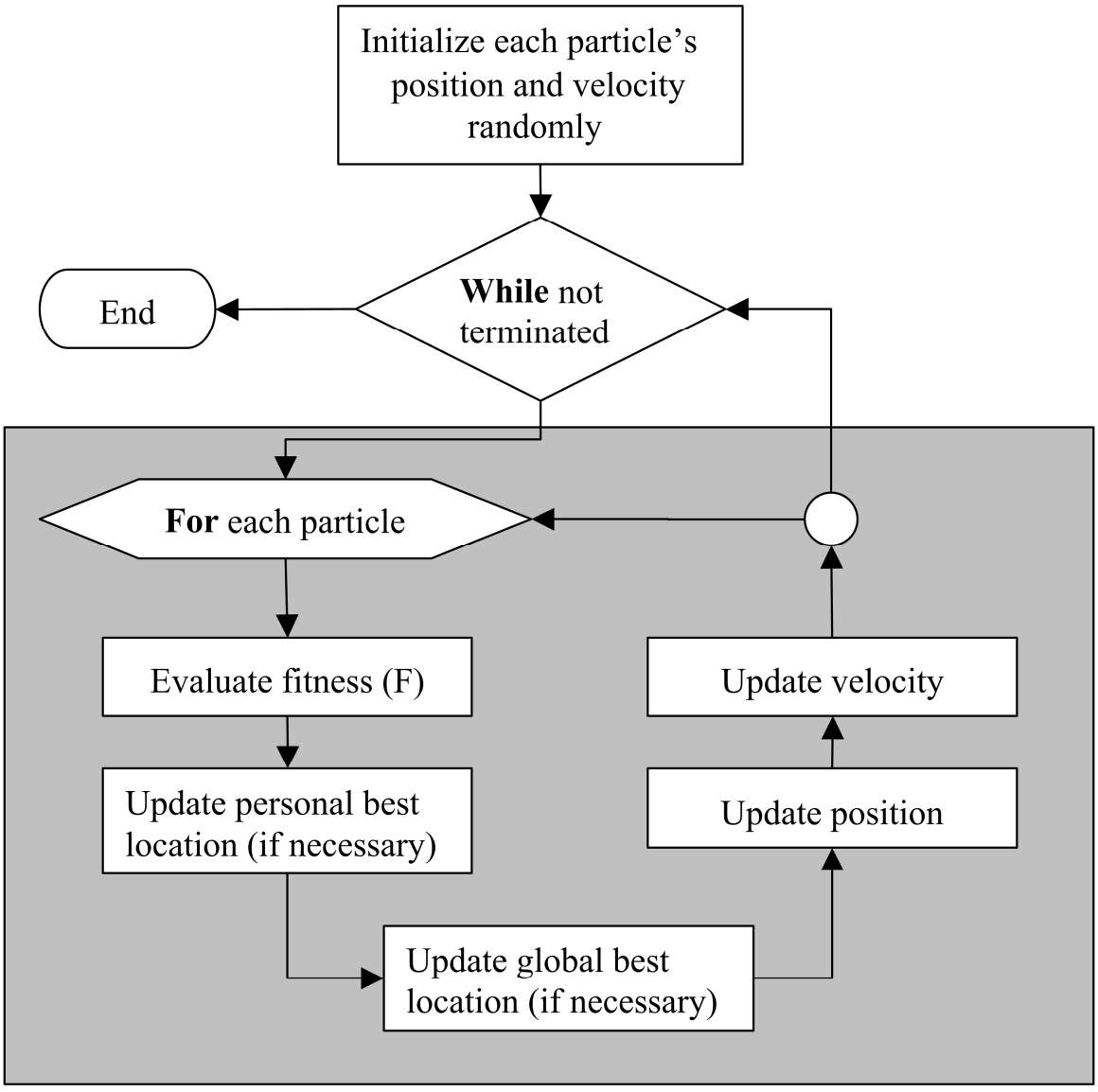

Figure 3: Flowchart illustrating the PSO algorithm. The number of loops iterated or the desired fitness being reached could be the terminating condition.

Figure 3 is a flowchart of the PSO algorithm. The starting position and velocity of each particle in the swarm is done randomly. After the swarm is initialized, the updating of position and velocity, at discrete intervals, is done as follows:

$$v_{i,new} = c_1 \cdot v_{i,old} + c_{\max} \cdot r_1 \cdot (\hat{x}_i - x_i) + c_{\max} \cdot r_2 \cdot (\hat{x}_{gi} - x_i)$$
$$x_{i,new} = x_{i,old} + v_{i,new}$$

- v and x are the velocity and position where the subscript i indicates the particular particle in the swarm and *old* and *new* indicate the current and future iteration
- c_1, and c_{max} are inertial constants
- r_1 and r_2 are random numbers between [0,1]
- $\hat{x}_i$ is the particle's best location so far
- $\hat{x}_g$ is the global best location seen by the swarm. This could be substituted with $\hat{x}_n$, neighborhood best, if neighborhoods are being used instead

The problem now is how does one determine a location, meaning a possible solution, is better than another. Going back to the example, if the swarm is searching for food and one location has more than another location then it is a better location. As with other optimization methods, the notion of a fitness evaluation is used. The fitness evaluation is a number that rates how good or bad a location is with respect to the particular fitness that is being sought. In engineering, there are often many design criteria that are being optimized simultaneously and the question becomes how are all these often unrelated

goals to be combined as a single fitness value that correctly reflects the desired end. One method of doing this is to use the method of weighted aggregation which is calculated by

$$F = \sum_{i=1}^{N} w_i \cdot f_i$$

where N is the number of fitness factors, f_i is the value of the ith fitness factor, and w_i is a weighting coefficient set by the designer. This method is simple and effective, but, if the goals are unrelated to one another, the weighting coefficients require tuning.

II.3 OBJECTIVES OF RESEARCH

The research pursued in this project evaluated the effects of the different parameters mentioned previously and optimized them to produce a broadband dual linear polarized antenna. The research pursued a lightweight antenna that operates in the X-band, has a wide bandwidth, has low loss or perturbation of signal, and could be usable in an array.

The following objectives were pursued in this research:

- To determine a suitably thick, low permittivity dielectric substrate that allows for an impedance bandwidth of 30% at 10GHz
- To establish the length of the patch that centers the impedance bandwidth at 10GHz
- To determine the location of the input feed and type of impedance matching network that has a return loss of 10dB or greater over the antenna bandwidth

- To determine a feeding method that has an isolation between signal ports of 20dB or higher
- To establish a HFSS solution that is stable by either physical testing or solving the model with a numerical method other than finite element
- To investigate antenna elements in an array allow for scanning in two dimensions, ±30 degrees along one axis and ±15 degrees along the other axis

CHAPTER III

METHODOLOGY

All simulations were performed using Ansoft's HFSS v10.1 [13], which is a finite element method electromagnetic solving software program. This program was chosen due to the author's familiarity with it through an internship with Raytheon and also because models may be created using multiple variables. This makes geometry changes to the model easy and effortless. The copper designs on each Duroid substrate were done in the etching facility at Texas A&M University using standard photolithography techniques. All S-parameter measurements were done on an Agilent 8510C Network Analyzer. The antenna pattern measurements were performed in the anechoic chamber of Texas A&M's Electromagnetics and Microwave Laboratory. The PSO-HFSS program developed was coded in Python, a high level scripting language. The graphs were done using data exported from HFSS and imported into Microsoft Excel. TX-Line, a computer program from Applied Wave Research, was used to find the microstrip line width for various impedances.

CHAPTER IV

SIMULATION RESULTS AND DISCUSSION

IV.1 APERTURE COUPLED PATCH ANTENNA

First, a single patch antenna was modeled on a foam substrate coupled through an aperture in the ground plane with two different microstrip lines. The model was being optimized for an impedance bandwidth of 30% and an isolation of 20dB between the input ports.

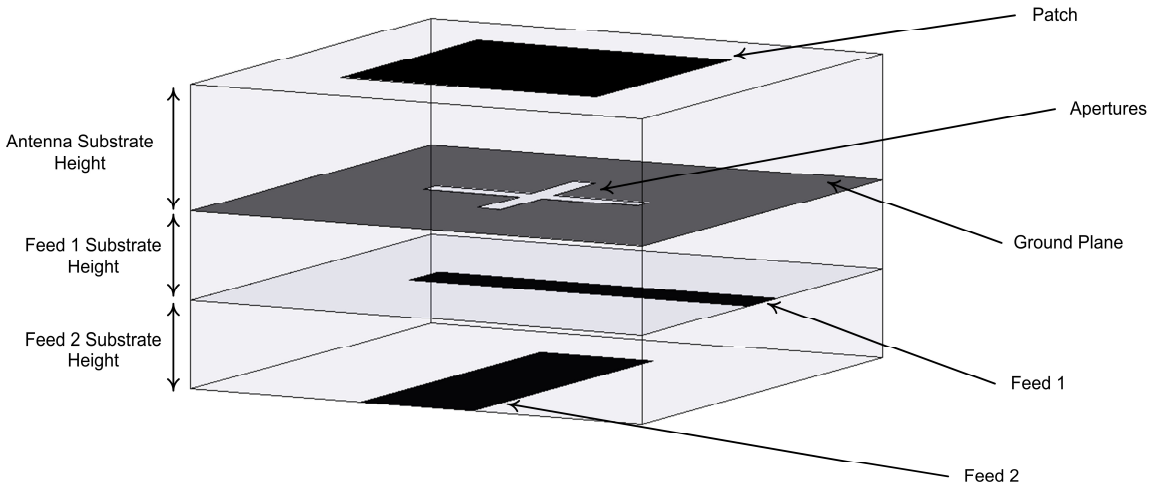

Figure 4: Geometry of a dual microstrip feed aperture coupled antenna. The 50 ohm microstrip lines were being fed through a rectangular aperture that is perpendicular to the line width with the combination being a cross shaped aperture.

This antenna used RT Duroid 5880 for the feed substrates. The substrate has a permittivity of 2.20 and a loss tangent of 0.0001. The substrate height of feed 2 (feed substrate 2) was 0.508mm and the substrate height of feed 1 (feed substrate 1) was also 0.508mm. This means that feed 1 is 0.508mm from the ground plane, and feed 2 is 1.016mm from the ground plane. The foam used as the antenna substrate had a permittivity of 1.06 and a height of 1.6mm or 3.2mm. Figure 4 shows the geometry for this initial antenna design.

It was determined that using dual offset feed lines, rather than a single feed line, to feed the aperture helped reduce the coupling and improve the impedance match [14]. **F**igure 5 shows a dual offset feed line. In the initial simulations, it was also found that this feed method increased the isolation between the two ports by about 8dB. A dual offset feed was two 100Ω lines connected by a simple power divider to a single 50Ω line. The widths of the lines for feed 1 were 1.6mm and 0.46mm for the 50 and 100Ω lines and was found using TX-Line [15], while the width of the lines for feed 2 were 3.2mm and 0.9mm for the 50 and 100Ω lines. A section of microstrip line was placed at the end of each feed line to facilitate the impedance match between the microstrip feed and the aperture.

Table 1: Variables used in the HFSS models along with their values.

Variable	Value	Variable	Value
Height feed substrate 1 (h_feed)	0.508mm	Feed 2 100 Ω line width (Wfeed2)	0.9mm
Height feed substrate 2 (h_feed2)	0.508mm	Feed 2 50 Ω line width (Wline2)	3.2mm
Height antenna substrate 1 (h_ant)	3.2mm	Offset feed line separation feed 1 (d_off)	2.5mm
Height antenna substrate 2 (h_ant2)	1.6mm	Offset feed line separation feed 2 (d_off2)	2.5mm
Feed 1 100 Ω line width (Wfeed)	0.46mm	Matching stub length feed 1 (L_feed_match)	5mm
Feed 1 50 Ω line width (Wline1)	1.6mm	Matching stub length feed 2 (L_feed_match2)	5mm
Length of aperture 1 slot (Lslot)	10mm	Length of aperture 2 slot (Lslot2)	10mm
Width of aperture 1 slot (Wslot)	1mm	Width of aperture 2 slot (Wslot2)	1mm
Midpoint width aperture 1 slot (Wslot_mid), bowtie aperture only	0.5mm	Midpoint width aperture 2 slot (Wslot_mid2), bowtie aperture only	0.5mm
Length patch 1 (Lpatch)	10.5mm	Length patch 2 (Lpatch2)	10.5mm

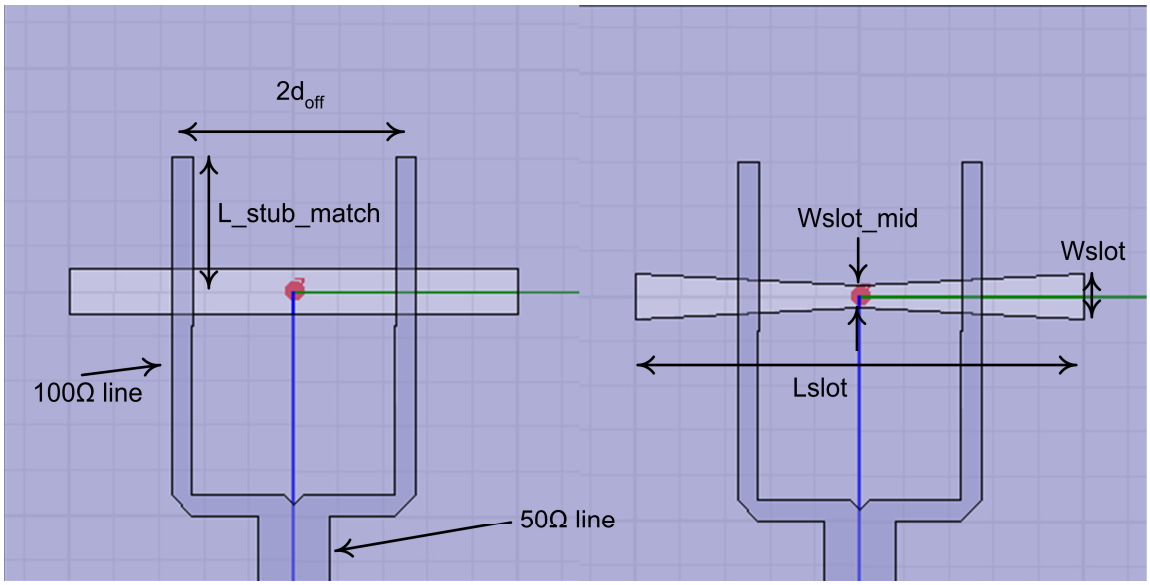

Figure 5: Geometry of dual offset microstrip feed line, left side, and bowtie aperture slot, right side, along with the associated variables used.

Equation (2) was used to find the initial width measurement to use in equation (3); both of these equations are found in the Background section. For a resonant frequency of 10GHz and the permittivity of the foam, the initial length of the microstrip patch was found to be 10.1mm. Substituting this new number as the width of the patch and repeating the process several times, the length of the initial square patch should be 10.5mm. By simulation, it was observed that the length for resonance at 10GHz was actually about 11.3mm. A rectangular aperture was used to couple the feed line to the antenna. By simulation, the best aperture dimensions found had a width of 1mm and a length of 9.5mm. At this point, the best bandwidth results were 7.5% at feed 1 and 10% at feed 2 as shown in Figures 6 and 7. The loops in the Smith chart show where the antenna and feed structure were resonant, and the nearer the loop to the center of the

chart the better the impedance match. In Figure 7 when the blue and red lines represent the Return Loss of both feeds. A return loss of 10dB and a VSWR of 2 are equivalent, so the portion of the graph below 10dB represents the bandwidth of the antenna. The third graph, in pink, was the isolation between the two feeds of the antenna and was below 20dB. The isolation over the bandwidth was acceptable but the bandwidth was too narrow.

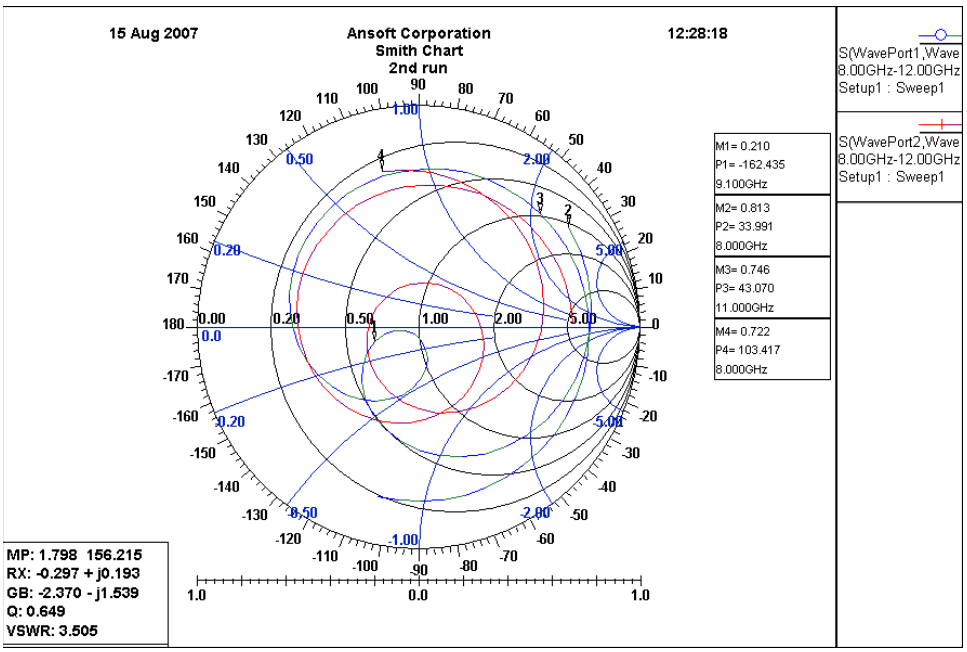

Figure 6: Smith chart of single patch dual feed aperture coupled antenna.

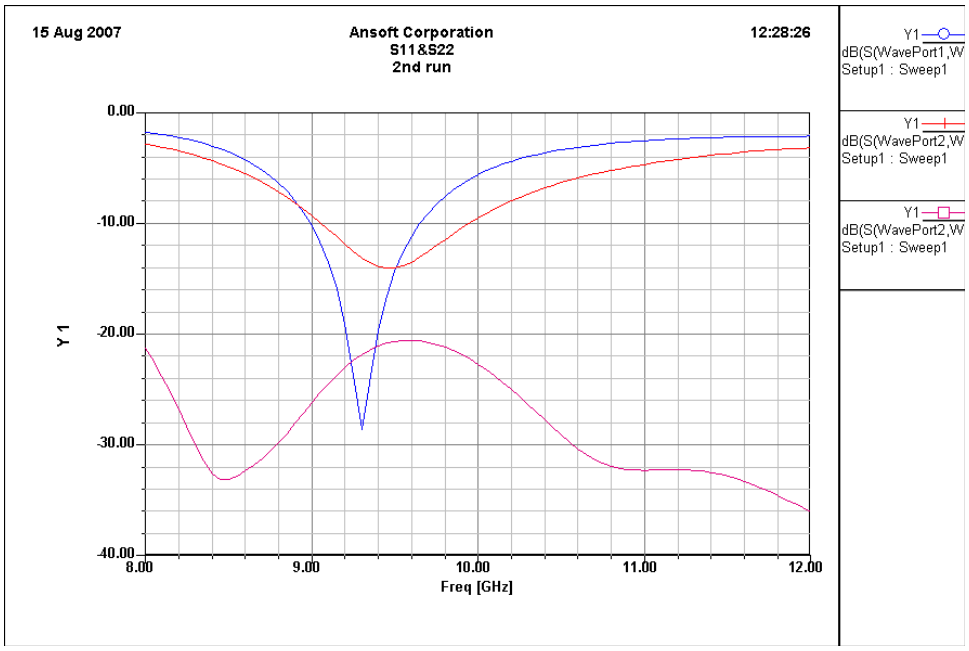

Figure 7: S parameter plot of single patch dual feed aperture coupled antenna.

A simplified model, using only feed 1, was implemented to study the effect of the aperture shape. With a bowtie aperture, the bandwidth was increased to 12.5%, an increase of 5%. Figure 5 shows the geometry of a bowtie aperture.

A different method to widen the bandwidth was to cut slots in the patch. Cutting slots in the patch has been shown to widen the bandwidth [1]; however, many of the shapes chosen were not suitable for use in a dual-linear polarized antenna. The shape chosen for symmetry was four L shaped slots, see Figure 8. These slots had very small effect on the bandwidth, but they did have a large effect on lowering the resonant size of the antenna.

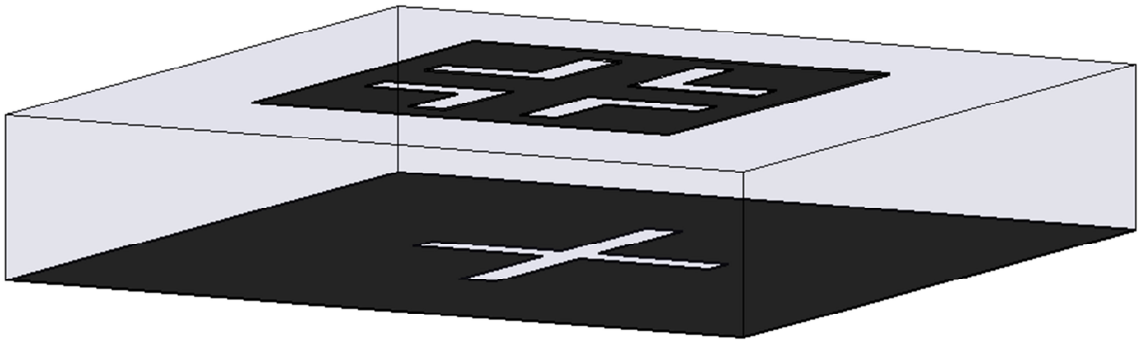

Figure 8: Geometry of the symmetric slots cut into the microstrip patch antenna over an aperture coupled feed.

The original design consideration was to keep the model as simple as possible and see if the bandwidth and isolation goals could be met. To that end, a single patch antenna was attempted. Although the 20dB isolation between ports has been met, the bandwidth of the antenna still falls short of the 30% desired. However, another way to increase the bandwidth was to introduce a second resonance in the impedance bandwidth that is offset from the first one. One way to do this would be to place a second patch antenna above the original antenna. This second antenna would be designed for a different resonant frequency. The coupling between the aperture and the two different resonant antennas should allow the bandwidth to be widened to 30%.

IV.2 STACKED PATCHES

This method of placing one patch antenna over another is known as stacked patch antennas. The first patch remained at a height of 3.2mm over the ground plane while the second patch was placed 1.6mm above the first one. The first time that this was done the second patch was 0.5mm smaller than the lower patch. Also since the bandwidth of the

two signals was comparable, the initial simulations of this aperture coupled stacked patch antenna was done with only one input to speed up the simulation. Using only one feed reduced the simulation time by about 60%. The bandwidth of the stacked patch was about double that of a single patch. However, the bandwidth was located at a lower frequency than before. Efforts to shift the bandwidth to the proper frequency range met with little success until the author employed the first rendition of the PSO-HFSS program, the Particle Swarm Optimization program. The initial PSO program was able to find two sets of antenna parameters, in the proper frequency range, with about 20% bandwidth. The first optimization by the PSO program had as variables the upper and lower patch dimensions as well as the length and widths of the bowtie aperture. A later version of the program, which worked more effectively, was able to find two sets of antenna parameters with 24% bandwidth. Figure 9 shows the comparison of the VSWR for the parameters found by the PSO programs.

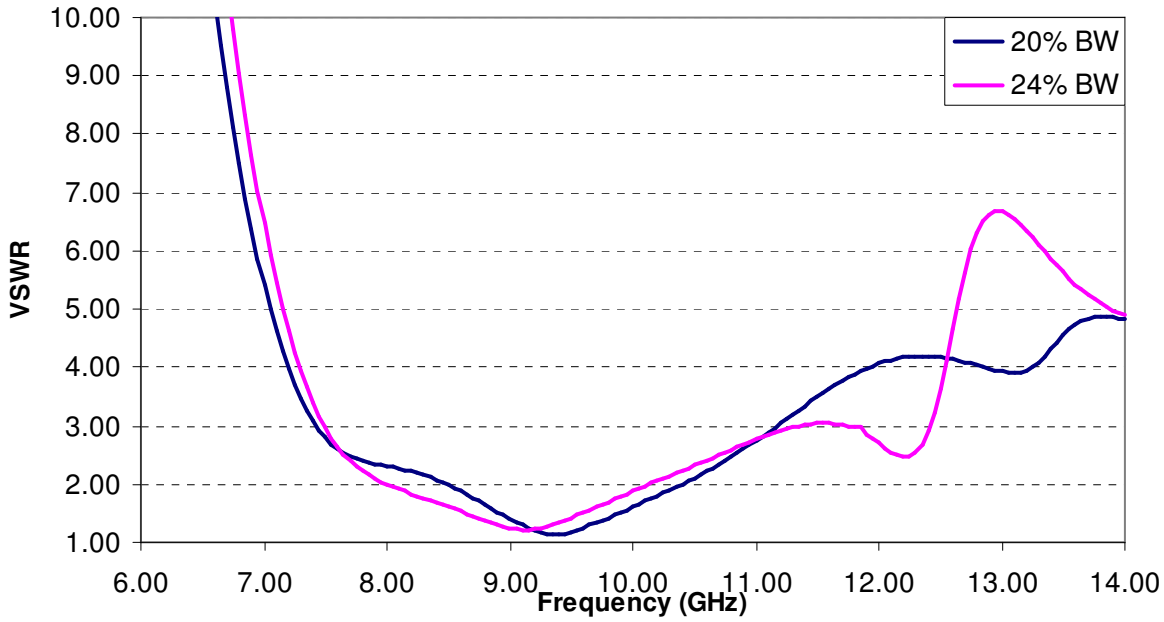

Figure 9: VSWR comparison of two different simulations for a single feed antenna with the microstrip at the feed 1 position for an aperture coupled stacked patch antenna.

The next step was to add the second feed back to the model. The second feed initially used a bowtie aperture 10mm long and 1mm wide which narrowed to 0.5mm at the middle. The initial simulation showed that the first input had a bandwidth of 14%, a decline from the 24% bandwidth found in the one feed model. The second input had a bandwidth of 23%. By reducing the matching stub length of feed 1 from 3mm to 2.4mm, the bandwidth was widened from 14% to 25%. In order to see if the bandwidth could be widened further, the two feed model was optimized with the PSO program. The program worked on optimizing the matching stub lengths for both feeds as well as feed 2's aperture parameters. After only a few runs, the bandwidth for both ports was widened;

the feed 1 bandwidth was increased from 25% to 33% while the feed 2 bandwidth was increased from 24% to 39%. These results can be seen in Figures 11 and 12.

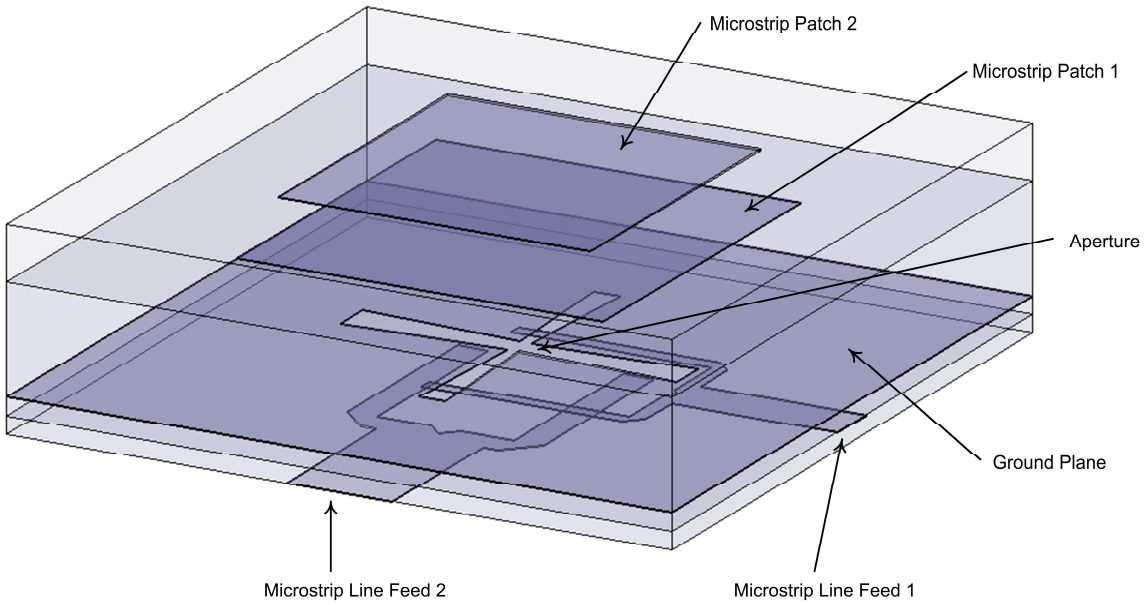

Figure 10: Geometry of the final aperture coupled stacked patch antenna with bowtie apertures and dual offset microstrip feed lines.

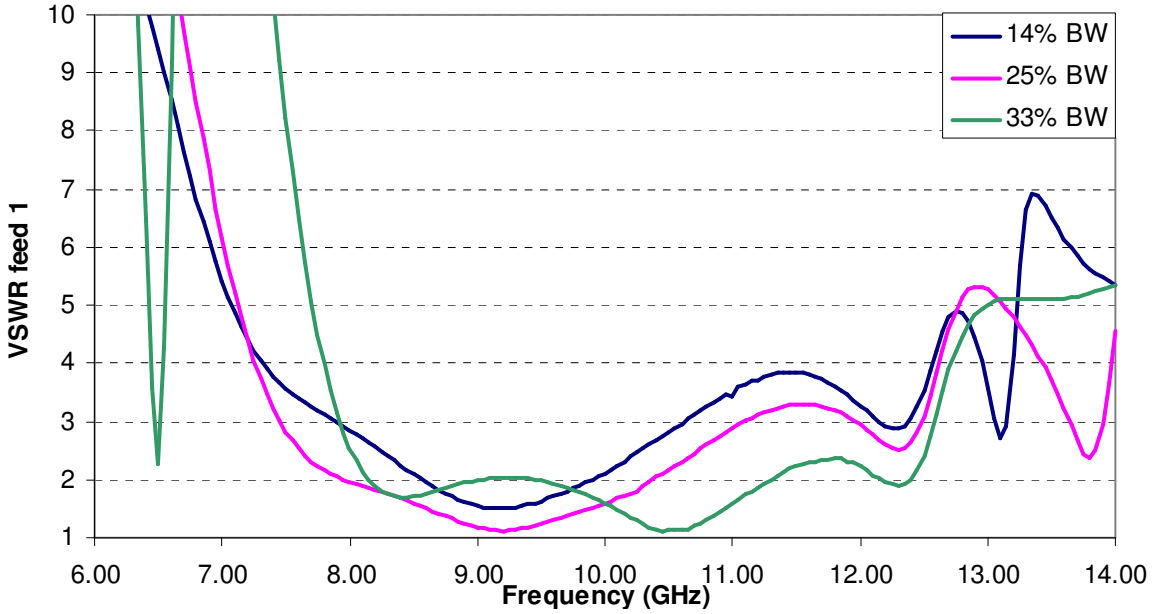

(a)

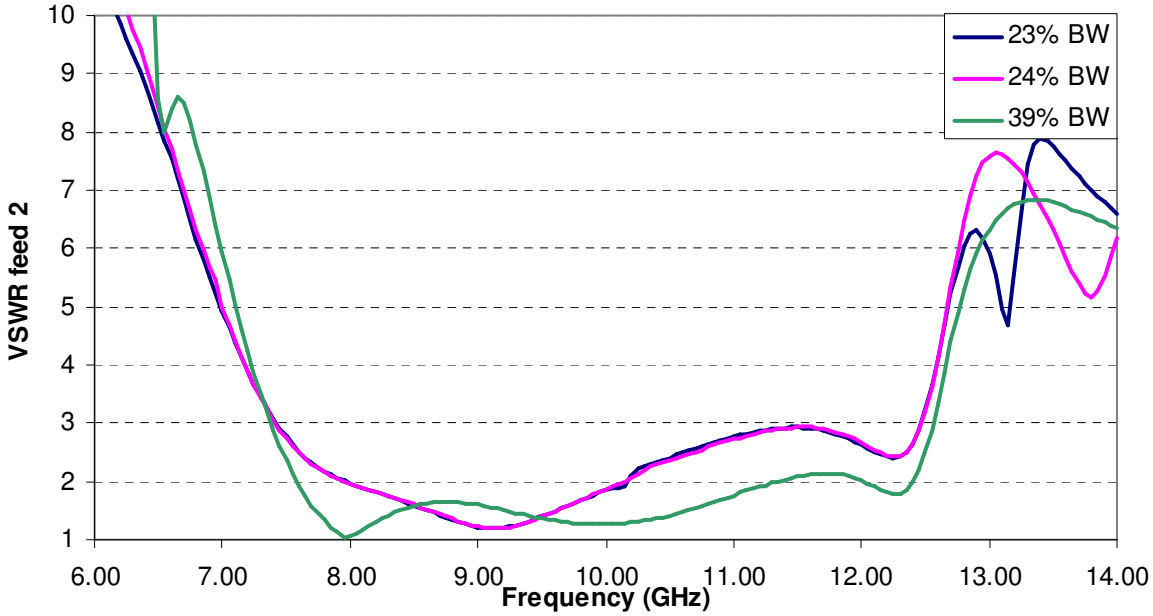

(b)

Figure 11: VSWR comparison for various sized patches, apertures, and matching stubs for the final aperture coupled stacked patch antenna with bowtie apertures and dual offset microstrip feed lines at feed 1, figure (a), and feed 2, figure (b).

IV.3 COAXIAL PROBE FED PATCH ANTENNAS

Another, simpler feed method explored was the probe feed. At the desired feeding location, a coaxial probe comes up through a hole in the ground plane with the center conductor continuing through the substrate and connecting to the microstrip patch. Although for this method of feeding a patch antenna is more sensitive to the feeding location, it does not have the alignment problems that are inherent in the multiple substrates used for an aperture coupled feed.

The patch dimensions as well as the antenna substrate were the same as previously described for the aperture coupled antenna. Using Equation (3), from the Background section, an initial feed location was chosen for a single probe. A single probe was used to reduce simulation time while the long probe was impedance matched.

The probe without any impedance matching had a very high impedance mismatch. One method attempted to offset the inductive mismatch was an annular ring gap around the probe feed, which showed good results with other antenna designs [8, 16]. A different method of impedance matching attempted was the L-shaped slots used in the aperture coupled antenna. However, the impedance match using the slots was not satisfactory enough to provide a usable bandwidth.

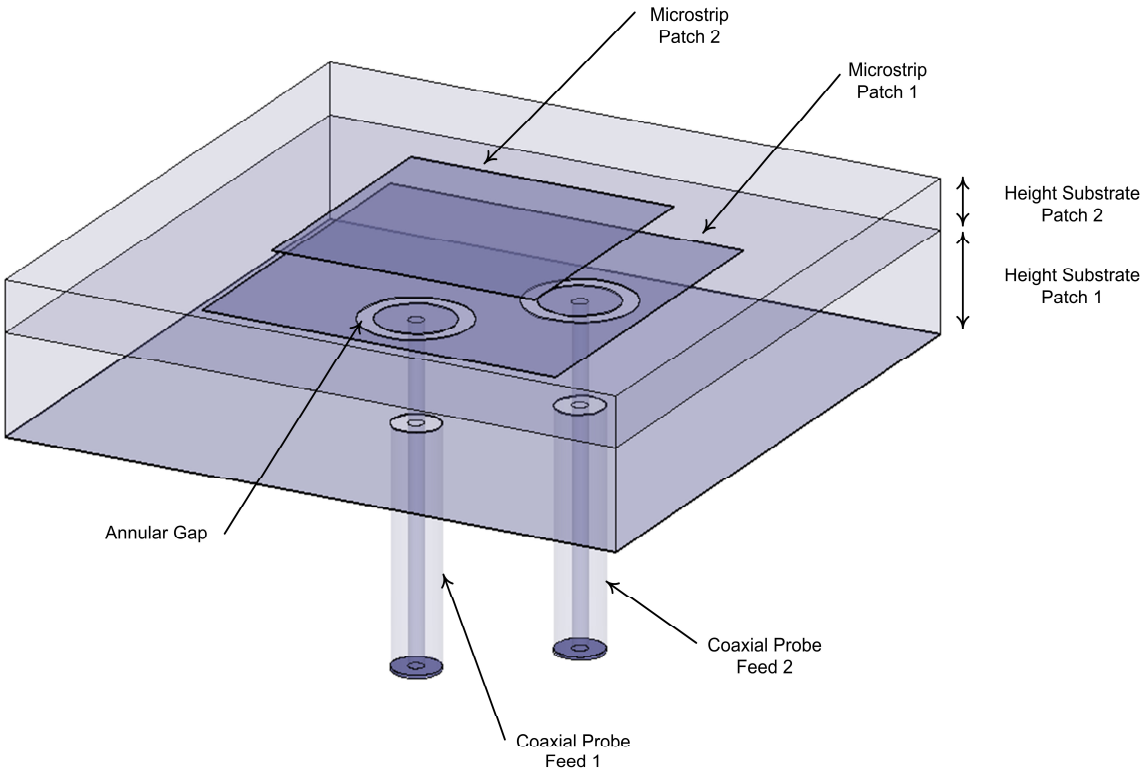

Figure 12: Geometry of coaxial fed stacked patch antenna with annular rings to impedance match long coaxial probe.

The method of stacked patches, tested with the aperture coupled feed, was also undertaken with a coaxial feed. Using the PSO-HFSS program, results were quickly forthcoming for a single coaxial feed stacked patch antenna. A set of antenna parameters with 40% bandwidth, the entire X-band, was found. However, when the second input was added to the model the isolation between the two feeds was around 10dB, which does not meet with the design criteria. A simple method to increase the isolation was not found so this line of approach was discontinued.

IV.4 PARTICLE SWARM OPTIMIZATION

The Particle Swarm Optimization algorithm was done in Python, a high level scripting language, to take advantage of the rapid prototyping that this language offers. Once the initial PSO code was completed it was tested with several benchmark functions for which solutions are known [12]. The PSO code was written to accept a reference to the function under optimization, which allows the problem to change without the need to change the PSO file.

The function sent to the PSO program did not actually solve the antenna model. HFSS was already being used to solve the antenna model so an interface between the PSO program and HFSS had to be developed. HFSS already had a built-in means to automate itself through Visual Basic (VB) Scripts. Using these scripts, models could be created, variables changed, models analyzed, or model solutions exported to a variety of formats. The first part of the function sent the locations generated by the swarm to a VB Script generator. The generator created a file that changed the variables to the current location, solved the model, and exported the results for that location to a file. The function then called HFSS and passed it the script file to execute. Once HFSS had finished solving the model, the exported result file could be analyzed. Rather than calling HFSS multiple times, the script file contained the instructions to solve for all the locations first and then allowed HFSS to quit so that the results could be analyzed.

The most difficult goal to achieve in this antenna design was the wide bandwidth located in the X-band. The fitness function reflected these two primary goals and was:

$$F = bandwidth\,(in\,\%) + 12.5 \cdot \left(\%\ X\ band\ \ in\ \ bandwidth\right)$$

The first goal was to determine the percent of bandwidth that the antenna had, and the second goal was to give a bonus based on the percent of the X-band occupied by the antenna bandwidth. This was the fitness function for the single feed antenna model. The dual feed antenna fitness function was very similar. The first difference was that the bandwidth had to meet the input isolation goal over the same bandwidth as the input impedance goal was met. The second difference was that the total fitness was just the sum of the fitness for each feed.

The first version of this PSO-HFSS program worked well and helped overcome some difficulties encountered in the antenna design. However, this version of the program had a flaw. The program was designed to output two extra files. The first was a log file that exported the location and fitness value of each particle in the swarm at every iteration of the PSO algorithm. The second file contained all the data needed to restart the PSO program if it were to unexpectedly quit or be manually terminated. Otherwise, the program would have to begin the optimization process from the beginning. In a review of the log files it was noted that some particles met with little success. Upon a further review of the swarm restart file, it was observed that those particles' best fitness and neighborhood best fitness values showed little improvement. This led to the discovery of a problem in the swarm communication. While a portion of the swarm was communicating, it was not communicating effectively, and the whole swarm was not communicating as well as it could. Once the communication problem was fixed, the PSO

program worked much better than before. This problem illustrates how valuable good communication is to Particle Swarm Optimization algorithms. Figure 14 shows how after the communication was fixed the average of all neighborhood fitness values approached that of the maximum fitness value, which was what was expected. The average of all neighborhood fitness values before the communication was fixed does not do this.

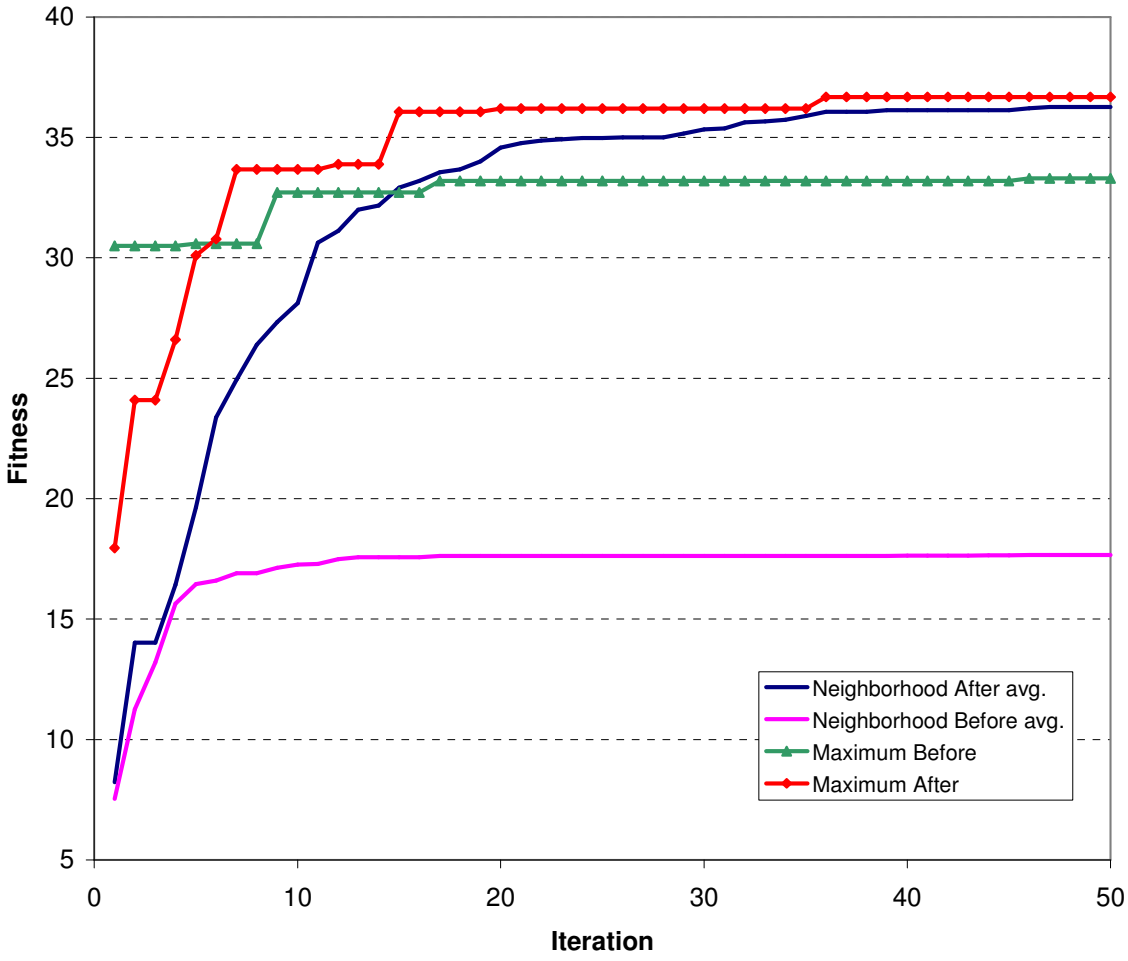

Figure 13: Average fitness value for the swarm neighborhoods as well as the maximum fitness value for the swarm before and after the swarm communication function was changed.

CHAPTER V

FABRICATION AND TESTING

The fabrication of the antennas was done with the substrates and foams described in the simulation section with the exception of the patch antennas. The patch antennas were etched on Duroid 3850 which has a dielectric constant of 3.2 and a thickness of 0.0508mm. Duroid 3850 was used because it has a low dielectric constant, it was also the thinnest substrate available, and it was an aid in aligning the various layers during construction.

Each substrate initially has a thin copper layer on both sides. The apertures in the ground plane, the feed lines, as well as the patch antennas must be etched into the copper of their respective substrates. This was done through photolithography.

Photolithography is the process used to selectively remove parts of a thin film. UV light was used to transfer a design from a photomask to a light-sensitive chemical, photoresist, on the substrate. A series of chemical treatments then revealed the design in the photoresist and etched away the copper unprotected by photoresist. The photomasks used were negatives created from the two dimensional copper geometries originating in the simulated model.

After all the copper layers have been etched, the next step was to cut two foam layers the same size as the ground plane. An SMA (SubMiniature version A, a type of coaxial rf connector) was soldered to the ground plane and the microstrip input line. For the two

feed antenna the second feed layer was bonded to the first feed layer before the second SMA connector was soldered. On the ground plane side, the 3.2mm thick layer of foam was layed down. Next, the first patch was layed down followed by a 1.6mm thick layer of foam and then finally the second patch. One side of the foam was adhesive backed, and a spray adhesive was used to bond the other layers to one another.

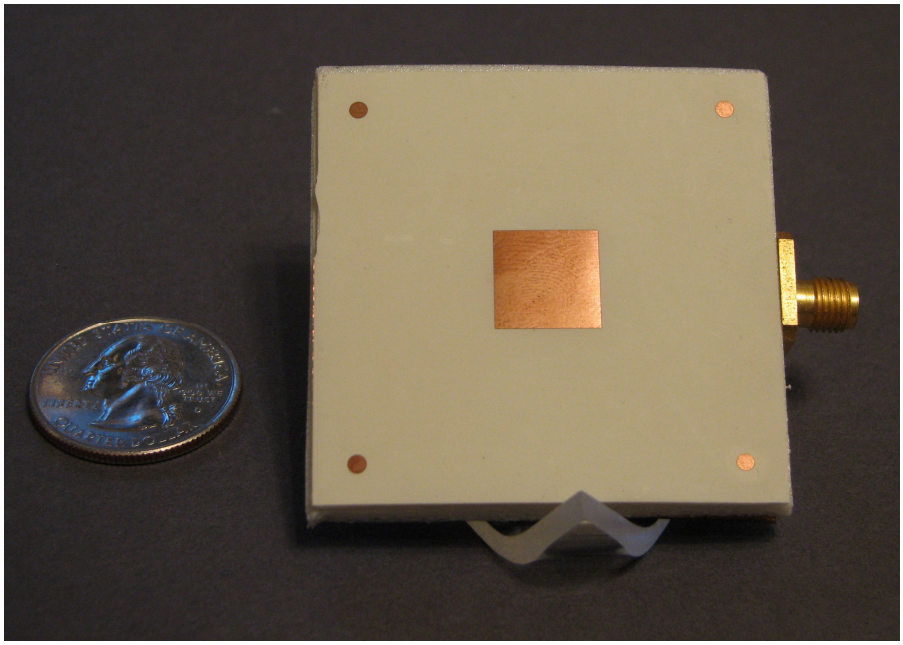

Figure 14: Picture of an intermediate design single feed stacked patch antenna coupled through a bowtie aperture. The quarter is a size reference and the four copper dots in the corners were for alignment during fabrication.

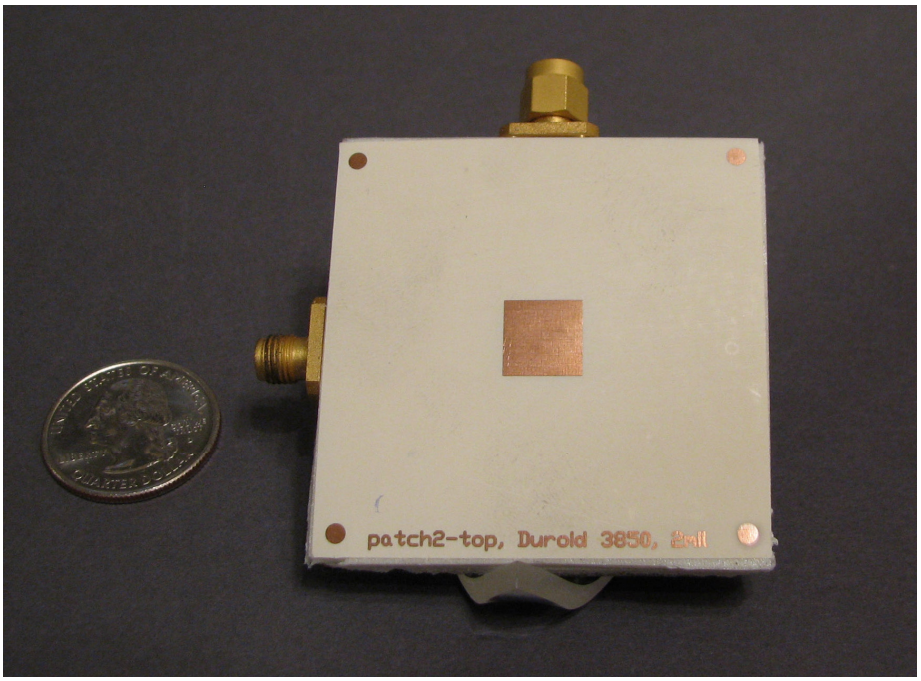

Figure 15: Picture of the final design dual feed stacked patch antenna coupled through a bowtie aperture. The quarter is a size reference and the four copper dots in the corners were for alignment during fabrication.

As shown in Figure 17 , the 2:1 bandwidth for the one port antenna was actually wider than what the simulation showed. The bandwidth was 31.5% at a center frequency of 8.75GHz. In Figures 18-20, the bandwidth for both feeds as well as the isolation between the feeds was compared to the simulated values. The bandwidth for feed 1 was 45.9% at a center frequency of 9.74GHz and the bandwidth for feed 2 was 45.1% at a center frequency of 10.18GHz. This was an increase of about 13% for feed 1 and 6% for feed 2 over the simulated bandwidth.

The radiation patterns were checked for several frequencies in the X-band. Three frequencies were chosen from the center of the dual feed antenna's bandwidth; these

frequencies were 9, 10, and 11GHz. Since the dual feed and single feed antenna bandwidths overlap at 9 and 10GHz the single feed antenna was measured at these two frequencies for comparison. In the plots of the radiation pattern "horizontal" is the E-plane cut and "vertical" is the cross-polarization. The antenna gain of the single feed and dual feed antennas constructed was between 5 and 10dB for all the frequencies measured. The cross-polarization levels were about 15dB below, or greater, than that of the main beam. A few of the cross-polarization plots were noisy so a fitted curve is included in the plot.

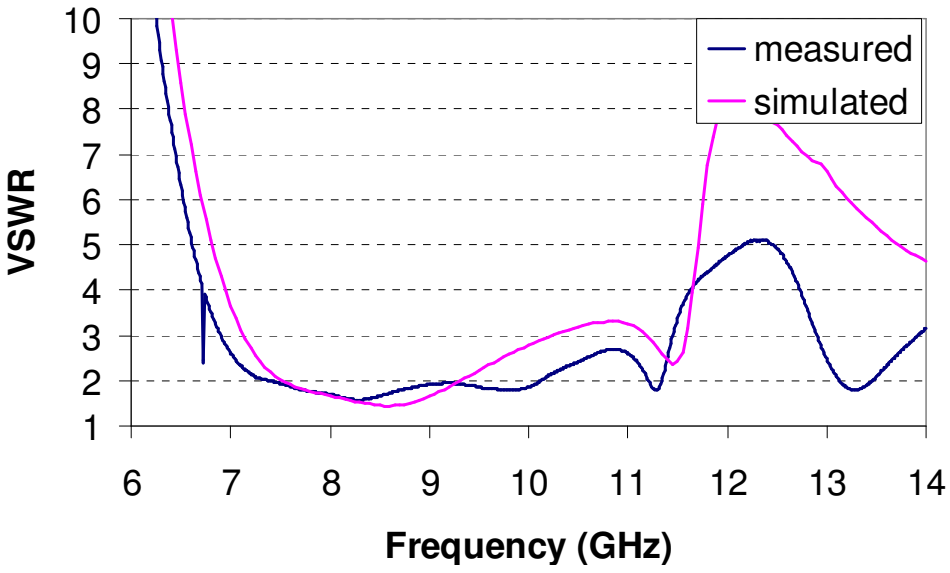

Figure 16: VSWR comparison of measured and simulated results for the intermediate design of the single feed aperture coupled stacked patch antenna.

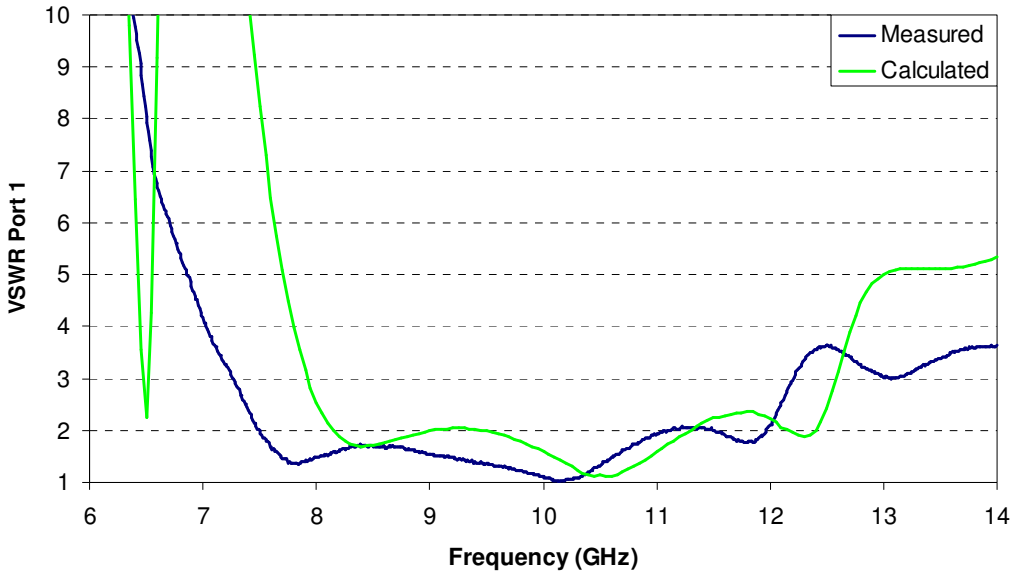

(a)

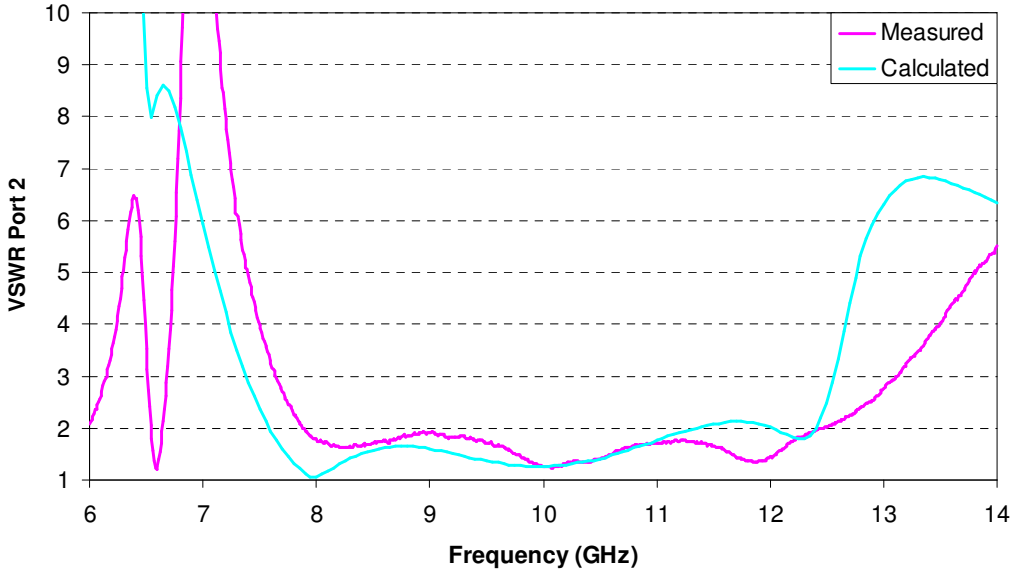

(b)

Figure 17: VSWR comparison of measured and simulated results for the final design of the dual feed aperture coupled stacked patch antenna at feed 1, figure (a), and feed 2, figure (b).

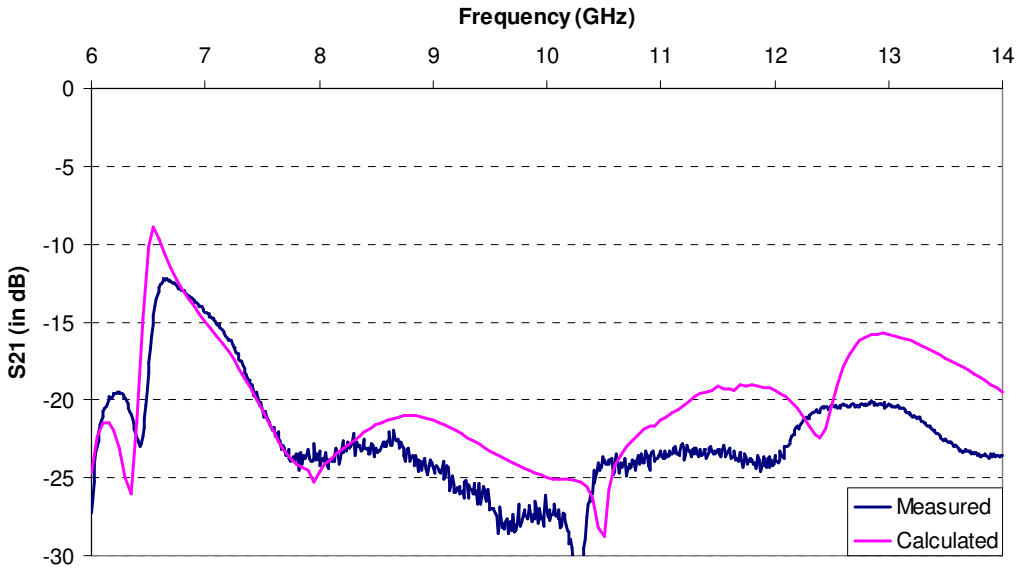

Figure 18: Isolation comparison between measured and simulated results for the final design of the dual feed aperture coupled stacked patch antenna.

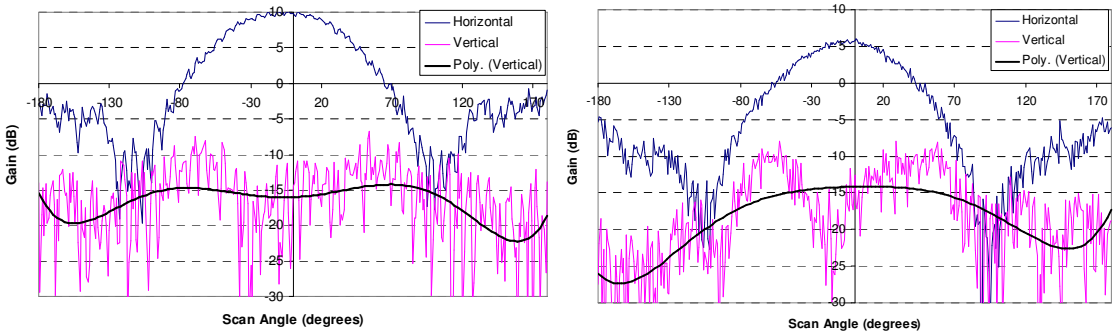

Figure 19: Antenna pattern at 9, left graph, and 10 GHz, right graph, for the intermediate design single feed antenna.

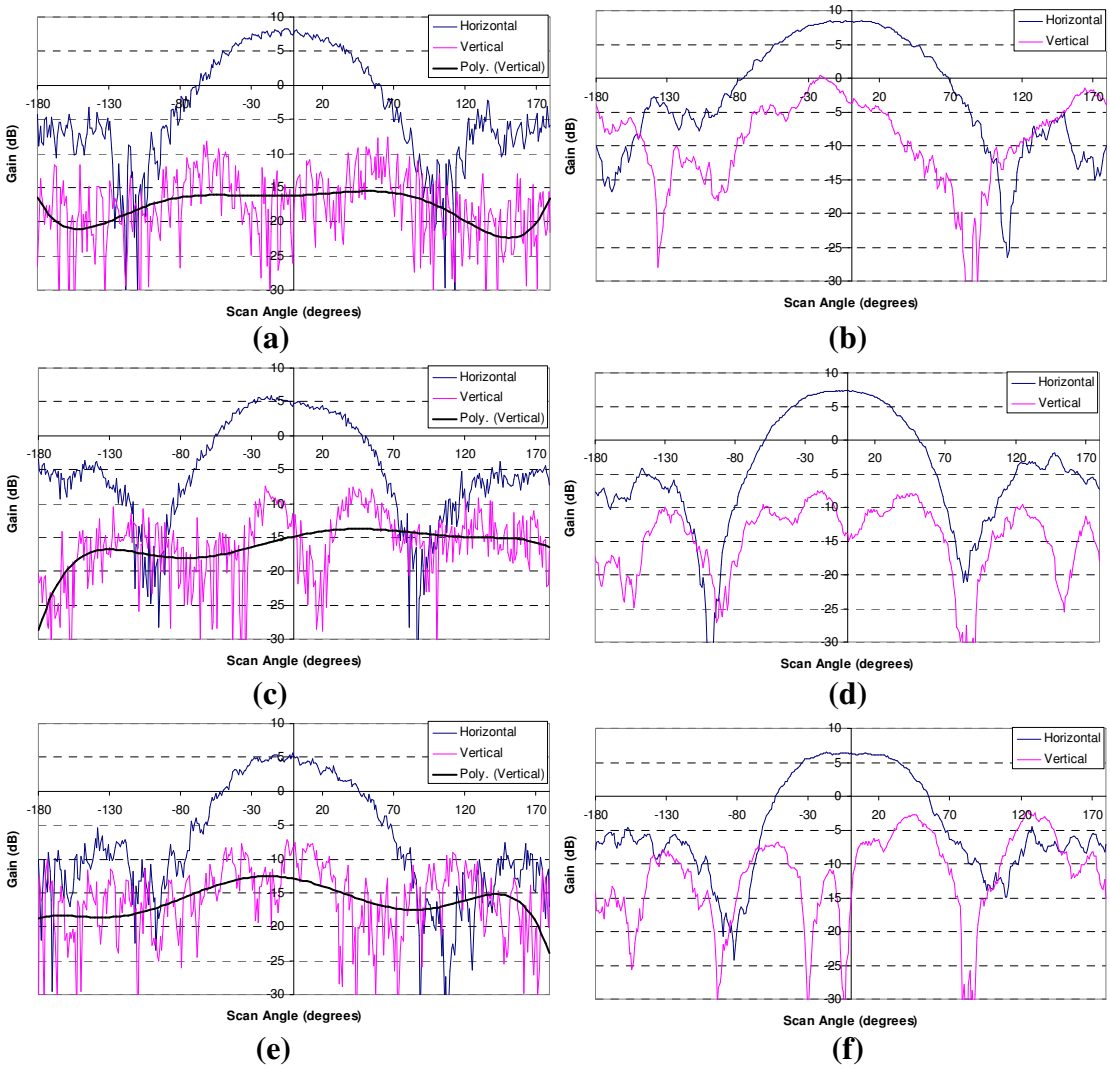

Figure 20: Antenna patterns at 9 GHz, figures (a) and (b), 10 GHz, figures (c) and (d), 11 GHz, figures (e) and (f), for the final design of the dual feed aperture coupled stacked patch antenna. Figures (a), (c), and (e) are for feed 1 while figures (b), (d), and (f) are for feed 2.

CHAPTER VI

CONCLUSIONS AND RECOMMENDATIONS FOR FUTURE WORK

As shown in the simulation and results sections, the isolation goal of -20dB has been met. This has been made possible by the method of impedance matching an aperture coupled antenna. Also, the shape of the aperture has been determined and found to have an effect upon the impedance bandwidth of the device. By using stacked patches, in conjunction with these other techniques, an impedance bandwidth of 45% for both linear polarizations was developed; this was 15% greater than the desired bandwidth. It was also shown that the antenna had good gain and low cross-polarization. The relatively new Particle Swarm Optimization algorithm was also successfully used in the design process. The algorithm allowed for a speedier optimization of the design variables than would otherwise have been possible. The time saved in this manner was put to use attempting more design possibilities. It was also demonstrated how social communication was key to the algorithm's function.

The antenna designed in this paper could be used in many applications. One area would be mobile communications. In this area, weight is always an issue, and the lightness of the antenna would be a boon. The dual-linear polarization would allow incoming signals to be received on one polarization and outgoing signals to be sent on the other polarization. The low profile of the antenna would allow for greater versatility in the

placement of the antenna on a vehicle. The regular pattern of the antenna should also facilitate the incorporation of the antenna into an antenna array.

Further improvement in wideband dual-linear polarized antennas should possibly focus on two new research areas. The first is fractal antennas and the second is Dielectric Resonant Antennas (DRA). Both of these topics show great promise for wideband antenna design using relatively simple structures.

REFERENCES

[1] R. Garg, P. Bhartia, I. Bahl, and A. Ittipiboon. *Microstrip Antenna Design Handbook*. 2nd ed. Norwood, Massachusetts: Artech House, 2001.

[2] V. Rathi, V., G. Kumar, and K. P. Ray, "Improved coupling for aperture coupled microstrip antennas," *IEEE Trans. Antennas Propagat.*, vol. 44, no. 8, pp. 1196-1198, August 1996.

[3] W. L. Stutzman, and G. A. Thiele. *Antenna Theory and Design*. 2nd ed. New York: John Wiley & Sons, 1997.

[4] C. A. Balanis, *Antenna Theory*, 3rd ed. New York: John Wiley & Sons Inc., 2005. 74.

[5] K. L. Lau, K M. Luk, and D. Lin. "A wide-band dual-polarization patch antenna with directional coupler." *IEEE Antennas and Wireless Propagation Letters,* vol. 1, pp 186-189, 2002.

[6] K. M. Luk, C L. Mak, R Chair, H Wong, and K F. Lee. "Microstrip antennas, broadband." *Encyclopedia of RF and Microwave Engineering*. 6 vols. New York: John Wiley & Sons Inc, 2005.

[7] Volakis, John L., *Antenna Engineering Handbook*, 4th ed. New York: McGraw-Hill, 2007.

[8] C. Borja, G. Font, S. Blanch and J. Romeu, "High directivity fractal boundary microstrip patch antenna," *IEEE Electronics Letters*, vol. 36, no. 9, pp. 778-779, April 2000.

[9] C. P. Baliarda, C. B. Borau, M. N. Rodero, and J. R. Robert, "An iterative model for fractal antennas: Application to the sierpinski gasket antenna," *IEEE Trans. Antennas Propagat*., vol. 48, no. 5, pp. 713-719, May 2000.

[10] Y. Rahmat-Samii, "Genetic algorithm (GA) and particle swarm optimization in engineering electromagnetic," *Applied Electromagnetics and Communications, 2003. ICECom 2003. 17 International Conference* on 1-3 Oct. 2003 pp 1-5.

[11] J. Robinson, and Yahya Rahmat-Samii. "Particle swarm optimization in electromagnetic," *IEEE Trans. Antennas Propagat.,* vol. 52, pp. 397-407, Feb. 2004.

[12] M. Clerc, *Particle Swarm Optimization*. London; Newport Beach: ISTE Ltd, 2006.

[13] *HFSS v10.1*. Computer software. Ansoft, LLC, 2006.

[14] S. D. Targonski, R. B. Waterhouse, and D. M. Pozar, "Design of wide-band aperture-stacked patch microstrip antenna," *IEEE Trans. Antennas Propagat.*, vol. 46, pp. 1245-1251, Sept. 1998.

[15] Applied Wave Research. (2007, June). TX-Line 2003. [Online]. Available: http://web.appwave.com/Products/Microwave_Office/TXLine.zip.

[16] P. S. Hall, "Probe compensation in thick microstrip patches," *IEEE Electronics Letters,* vol. 23, no. 11, pp. 606-607, May 1987.

VITA

Name:	Christopher B. Smith
Address:	Texas A&M University Department of Electrical Engineering 214 Zachry Engineering Center College Station, Texas 77843-3128
E-mail Address:	mcanjo@gmail.com
Education:	B.S., Electrical Engineering, Texas A&M University, 2005 M.S., Electrical Engineering, Texas A&M University, 2008